

1           **Impact of meteorological conditions on BVOC emission rate from Eastern**  
2                                   **Mediterranean vegetation under drought**

3

4   Qian Li<sup>1,2</sup>, Gil Lerner<sup>2</sup>, Einat Bar<sup>3</sup>, Efraim Lewinsohn<sup>3</sup>, Eran Tas<sup>2\*</sup>

5   <sup>1</sup> School of Ecology, Hainan University, No 58, Renmin Avenue, Haikou, Hainan province,  
6   China

7   <sup>2</sup> Institute of Environmental Sciences, The Robert H. Smith Faculty of Agriculture, Food and  
8   Environment, The Hebrew University of Jerusalem, P.O. Box 12, Rehovot 7610001, Israel

9   <sup>3</sup> Department of Vegetable Research, Agricultural Research Organization – Newe Ya'ar Center,  
10   Israel

11

12

13

14

15   \* Correspondence to:

16   Eran Tas, Institute of Environmental Sciences, The Robert H. Smith Faculty of Agriculture, Food  
17   and Environment, The Hebrew University of Jerusalem, P.O. Box 12, Rehovot 7610001, Israel  
18   [eran.tas@mail.huji.ac.il](mailto:eran.tas@mail.huji.ac.il)

19 **Abstract**

20 A comprehensive characterization of drought's impact on biogenic volatile organic  
21 compounds (BVOC) emissions is essential for understanding atmospheric chemistry under  
22 global climate change, with implications for both air quality and climate model simulation.  
23 Currently, the effects of drought on BVOC emissions are not well characterized. Our study  
24 aims to test: i) whether instantaneous changes in meteorological conditions can serve as a  
25 better proxy for drought-related changes in BVOC emission compared to the absolute  
26 values of the meteorological parameters, as indicated in a companion article based on  
27 BVOC mixing-ratio measurements; ii) the impact of a plant under drought stress receiving  
28 a small amount of precipitation on BVOC emission rate, and on the manner in which the  
29 emission rate is influenced by meteorological parameters. To address these objectives, we  
30 conducted our study during the warm and dry summer conditions of the Eastern  
31 Mediterranean region, focusing on the impact of drought on BVOC emissions from natural  
32 vegetation. Specifically, we conducted branch-enclosure sampling measurements in Ramat  
33 Hanadiv Nature Park, both under natural drought and after irrigation (equivalent to 5.5–7  
34 mm precipitation), for six selected branches of *Phillyrea latifolia*, the highest BVOC  
35 emitter in this park, in September–October 2020. The samplings were followed by gas  
36 chromatography-mass spectrometry analysis for BVOCs identification and flux  
37 quantification. The results corroborate the finding that instantaneous changes in  
38 meteorological parameters, particularly relative humidity (RH), offer the most accurate  
39 proxy for BVOC emission rates under drought, compared to the absolute values of either  
40 temperature (T) or RH. However, after irrigation, the correlation of the detected BVOC  
41 emission rate with the instantaneous changes in RH became significantly more moderate,

42 or even reversed. Our findings highlight that under drought, the instantaneous changes in  
43 RH, and to a lesser extent in T, are the best proxy for the emission rate of monoterpenes  
44 (MTs) and sesquiterpenes (SQTs), whereas under moderate drought conditions, T or RH  
45 serves as the best proxy for MT and SQT emission rate, respectively. In addition, the  
46 detected emission rates of MTs and SQTs increased by 150% and 545%, respectively, after  
47 a small amount of irrigation.

48

## 49 **1 Introduction**

50 Biogenic volatile organic compounds (BVOCs) are released by plants and other organisms  
51 to the atmosphere. They play a critical role in both climate change and photochemical air  
52 pollution (Cai et al., 2021; Calfapietra et al., 2013; Curci et al., 2009; Guenther, 2013;  
53 Kesselmeier and Staudt, 1999; Peñuelas et al., 2009). BVOCs are thought to be emitted by  
54 plants as a defense mechanism against biotic and abiotic stresses, such as herbivory and  
55 high temperatures (Berg et al., 2013; Blande et al., 2007; Brilli et al., 2009; Peñuelas and  
56 Munné-Bosch, 2005). BVOCs may also be involved in plant–plant and plant–animal  
57 communication, allowing plants to signal to other organisms about their response to  
58 environmental conditions (Baldwin et al., 2006; Filella et al., 2013; Niinemets and Monson,  
59 2013).

60 The emission rate and composition of BVOCs can vary widely depending on  
61 various factors, such as meteorological conditions, rate of synthesis, and physicochemical  
62 properties (Niinemets and Monson, 2013). Climate change is expected to significantly  
63 impact BVOC emission rate and composition. As temperature rises, the emission rate of  
64 most BVOCs increases in an Arrhenius-type manner (Goldstein et al., 2004; Greenberg et

65 al., 2012; Guenther et al., 1995; Monson et al., 1992; Niinemets et al., 2004; Tingey et al.,  
66 1990). On the other hand, drought can have a more complex effect on the emission and  
67 composition of BVOCs. Depending on the type of vegetation, the level of drought stress,  
68 and additional ambient conditions, the emission of BVOCs can be partially or completely  
69 suppressed (Fortunati et al., 2008; Holopainen and Gershenzon, 2010; Llusia et al., 2016;  
70 Peñuelas and Staudt, 2010; Schade et al., 1999), or enhanced in a way that has not yet been  
71 characterized (Fitzky et al., 2023; Geron et al., 2016; Potosnak et al., 2014).

72 The effect of drought on isoprene emission has been extensively studied, and it was  
73 discovered to be postponed relative to, and/or less significant than the effect on  
74 photosynthetic rate (Asensio et al., 2007; Brillì et al., 2007; Fortunati et al., 2008; Pegoraro  
75 et al., 2006; Ryan et al., 2014). However, whereas under moderate drought stress, isoprene  
76 emission may only slightly decrease or increase, it was shown to decrease considerably  
77 under severe or prolonged drought stress (Fortunati et al., 2008; Han et al., 2022; Jiang et  
78 al., 2018). The impact of drought on the emission of other BVOCs, such as monoterpenes  
79 (MTs) and sesquiterpenes (SQTs), has been less studied.

80 The Eastern Mediterranean has a unique climate characterized by a hot and dry  
81 summer, making it an ideal location to study the impact of drought on BVOC emissions.  
82 The semiarid and arid regions are particularly vulnerable to climate change, and climate  
83 simulations predict that the Eastern Mediterranean region will experience more frequent  
84 and severe droughts in the future (Giorgi and Lionello, 2008; Lionello, 2012). Research  
85 conducted in Israel has investigated the impact of drought on BVOC emissions from a  
86 range of local plant species. For example, Llusia et al. (2016) examined the effect of  
87 drought on terpene emission from Yatir Forest, a pine forest in the northern Negev. They

88 found that some of the MT and SQT emissions increased under moderate drought  
89 conditions but strongly decreased under severe drought conditions. Another measurement  
90 by Li et al. (2024), performed in late autumn 2016 in Shibli Forest in northern Israel, found  
91 that under severe drought stress, BVOC emissions respond more significantly to the  
92 instantaneous changes in meteorological parameters (especially relative humidity [RH])  
93 than to the meteorological parameters themselves. These studies suggest that the impact of  
94 drought on BVOC emissions is not well-characterized and varies in a complex manner,  
95 depending on plant species, BVOC type, and meteorological parameters, such as  
96 temperature (T) and RH, as well as the level of drought stress. Hence, more research is  
97 needed to better characterize the effect of drought on BVOC emission rates and  
98 composition, which can in turn improve air quality and climate modeling.

99 In this study, we use the severe drought conditions during the autumn in the Eastern  
100 Mediterranean to study the effect of drought on the emission of BVOCs from natural  
101 vegetation. The main specific objectives of this study were to: i) identify whether  
102 instantaneous changes in meteorological parameters can serve as a better proxy for BVOC  
103 emission rates under drought than their absolute values, and ii) determine the extent to  
104 which small precipitation amounts, under drought conditions, can impact BVOC emission  
105 rates and the manner in which the emission rate is influenced by meteorological parameters.

106

## 107 **2 Methods**

108 We used an enclosure-based measurement system to quantify BVOC emissions, allowing  
109 for direct measurement of BVOC fluxes at the branch level. The measurements were  
110 performed in autumn under the prolonged drought stress conditions typical to this region.

111 BVOC measurements in the Eastern Mediterranean are rare, and to the best of our  
112 knowledge, our study is the first to apply direct measurements of BVOC flux from specific  
113 branches of natural vegetation in this region. Plants were sampled before and after the  
114 application of a small amount of irrigation to study the response of BVOC emissions, under  
115 exposure to natural drought conditions, to a small amount of precipitation. This was  
116 followed by gas chromatography–mass spectrometry (GC–MS) to identify and quantify  
117 the emitted BVOCs. Closed chambers are often used for measurements of BVOCs at the  
118 branch level (Duhl et al., 2008). Compared to open-system methods, the enclosure-based  
119 system (including a glass cuvette or Tedlar bag) can focus on specific vegetation in a more  
120 controlled manner. To investigate the effects of drought on BVOC emission rates and  
121 composition, we performed two sets of measurements – before and after irrigation – for  
122 comparison. To study the effect of meteorological conditions on BVOC flux, we monitored  
123 meteorological parameters inside the bag and at a meteorological station that was 300–600  
124 m from the branches.

125

## 126 *2.1 Sampling site and studied species*

127 The on-site branch measurements were conducted at Ramat Hanadiv Nature Park (32°  
128 33' 19.87" N, 34° 56' 50.23" E), 3.6 km from the Eastern Mediterranean seashore and  
129 exposed to a typical Eastern Mediterranean climate, with annual precipitation of 640 mm  
130 (averaged over the last 5 years, and occurring mainly between November and March). The  
131 vegetation at the site is dominated by mixed Mediterranean shrubbery. More details about  
132 the site and vegetation can be found in Li et al. (2018) and Dayan et al. (2020). The  
133 measurements were conducted at the end of summer/beginning of autumn under drought

134 conditions. No precipitation was recorded for 108 days between 24 May 2020 and the  
135 beginning of the study on 9 Sep 2020.

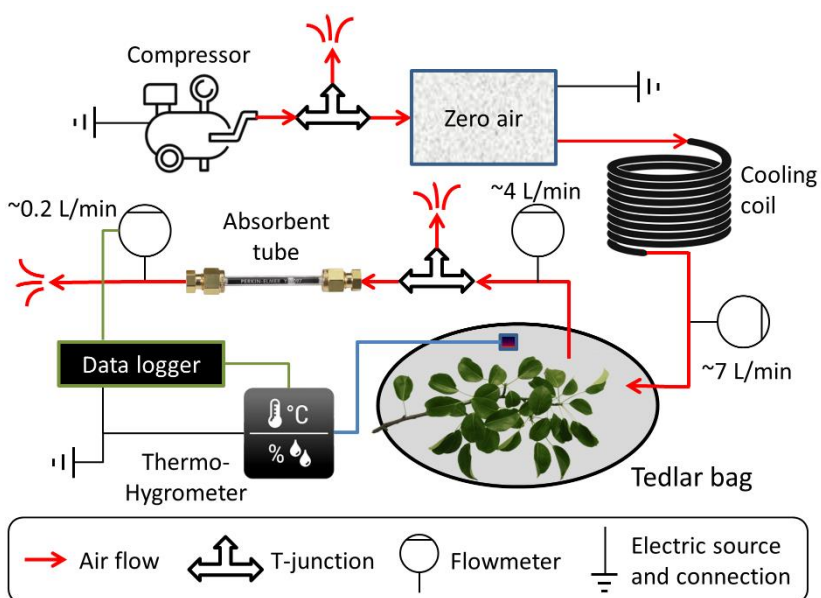
136 *Phillyrea latifolia* (broad-leaved phillyrea), identified as the greatest BVOC-  
137 contributing plant species in the Ramat Hanadiv natural park, was sampled. The species is  
138 native to the Mediterranean Basin and belongs to the family Oleaceae. In Ramat Hanadiv,  
139 it accounts for 7.5% of all vegetation, but up to ~35% of all BVOC emissions, according  
140 to the Model of Emissions of Gases and Aerosols from Nature (MEGAN v2.1; Dayan et  
141 al., 2020; Guenther et al., 2012; Li et al., 2018). The selected plants were mature and did  
142 not show any visible signs of senescence. Sampled branches were shaded, to eliminate the  
143 effect of non-natural high temperature in the enclosure system, and measurements were  
144 performed at 1.5 to 2 m aboveground.

145

## 146 ***2.2 Branch-enclosure sampling system and setup***

147 Figure 1 presents a self-made branch-sampling system was used for this study. All tubes  
148 and connections are Teflon, while valves and flowmeters are stainless steel. A compressor  
149 provides a controllable rate of ambient air flow through an adjustable T-junction valve (to  
150 adjust the flow rate) to a zero-air device (Model 1150 dual reactor, Thermo Fisher  
151 Scientific, Waltham, MA, USA), which includes a catalytic converter heated to ~350 °C to  
152 oxidize carbon monoxide (CO) and hydrocarbons (HC) to carbon dioxide (CO<sub>2</sub>) and water  
153 (H<sub>2</sub>O). From the zero-air device, the air flows through a copper coil to cool it down, and  
154 then through a mass flowmeter into a Tedlar bag (CEL Scientific Corporation, Cerritos,  
155 CA, USA), at a flow rate of about 7 L min<sup>-1</sup> (monitored by flowmeter A), a high enough  
156 inflow to produce slight overpressure inside the bag. The inert and light-transparent 10 L

157 Tedlar bag is tied tightly around a tree branch, along with an EL-MOTE-TH temperature  
 158 and RH sensor (Lascar Electronics, Whiteparish, Wiltshire, UK). The outlet airflow ( $\sim 4$  L  
 159  $\text{min}^{-1}$  monitored by flowmeter B) is directed to the C2-CAXX-5032 hydrophobic inert-  
 160 coated stainless-steel adsorbent tube (CSLR, Markes International, Llantrisant, UK) filled  
 161 with a mixture of Tenax TA and Carbograph as adsorbent, at a rate of  $\sim 0.2$  L  $\text{min}^{-1}$   
 162 (monitored by flowmeter C), regulated by the T-junction valve downstream of flowmeter  
 163 B. The flow rate through the adsorbent tube, as well as T and RH were recorded with a  
 164 CR1000 data logger (Campbell Scientific, Logan, UT, USA).



165 **Figure 1.** Schematic of the branch-enclosure sampling system. VOCs are removed from the ambient air  
 166 before entering a transparent Tedlar bag and an adsorbent tube to monitor BVOC emissions from the enclosed  
 167 branch, using a flow-controlled system (see Sect. 2.2).

168

### 169 **2.3 Analytical quantification of the sampled BVOCs**

170 A Centri™ (Markes International) preconcentration system was used to desorb the tubes  
 171 into the cold trap (graphitized carbon trap; used for sampling VOCs of C4/5 to C30/32)  
 172 under the following conditions: desorption for 5 min at 280 °C with a trap flow of 30 mL



173 min<sup>-1</sup>. Desorption of trap was at a rate of 20 °C s<sup>-1</sup> to 300 °C into an Agilent GC–MS  
174 (7890A/5975C) system (Santa Clara, CA, USA) equipped with a Stabilwax column  
175 (Restek, 30 m, 0.25 mm ID capillary column; polyethylene glycol, 0.25 µm film thickness).  
176 The general run parameters were as follows: injector, 230 °C; column oven, initial  
177 temperature of 45 °C for 5 min, followed by a ramp of 5 °C min<sup>-1</sup> to 120 °C, 20 °C min<sup>-1</sup>  
178 to 240 °C final, and 5-min hold with a total run time of 31.5 min; carrier gas, He 32 psi;  
179 mass spectrometer ionization energy, 70 eV; m/z, 41 to 300; scan time, 5.4 s. The  
180 chromatograms were analyzed using MassHunter Quant Analysis (B.10.00, Agilent  
181 Technologies, Santa Clara, CA, USA) software. Compounds were identified by comparing  
182 their relative retention indices and mass spectra with those of authentic standards or those  
183 found in the literature, supplemented with W10N14 and 2205 GC–MS libraries.

184 We chose to analyze the most abundant BVOC species: *cis*-β-ocimene (E, Z) (MT),  
185 and β-caryophyllene, α-humulene, α-farnesene, germacrene-D (SQTs). For calibration,  
186 analytical-grade standard solutions (7–12 concentrations) were prepared, ranging in  
187 concentrations from 0.25 to 1000 ng mL<sup>-1</sup> by diluting known masses of pure chemicals  
188 with methanol. The calibration analytes were injected using a GC syringe onto clean  
189 sorbent tubes connected to a calibration solution-loading rig (Markes International) at a  
190 nitrogen flow of 80 mL min<sup>-1</sup> for 5 minutes. The standards for the BVOC species were *cis*-  
191 β-ocimene (E, Z) (W353977, Sigma-Aldrich) (MT), and β-caryophyllene (22075-1ML-F,  
192 Sigma-Aldrich), α-humulene (PHL83351, Sigma-Aldrich), α-farnesene (Biosynth®  
193 Carbosynth Ltd., UK), germacrene-D (Toronto Research Chemicals, Canada) (SQTs),  
194 according to the most abundant species (see Sect. 2.4). The sampled solution was mixed  
195 with 5 µL of each compound in the solvent. All standard-loaded tubes were prepared in

196 triplicate and results were averaged. The loaded tubes were analyzed under the same  
197 conditions used for the other samples. Standard curves of peak area counts vs. VOC mass  
198 ( $\mu\text{g}$ ) were fitted using linear regression analyses; both yielded high regression coefficients  
199 ( $r^2 \geq 0.99$  in most cases). More details on the calibration are provided in Sect. S1. For the  
200 minor MTs and SQTs, the calibration curve of *cis*- $\beta$ -ocimene (E, Z) and the averaged  
201 calibration curve of the four most abundant SQTs were used for a rough estimation of their  
202 emission rates.

203

## 204 ***2.4 Experimental setup***

### 205 ***2.4.1 Branch sampling, meteorological parameter measurements and flux evaluation***

206 The field measurements were performed from late summer to early autumn – 9 Sep to 27  
207 Oct 2020. Samplings were conducted on six selected *Phillyrea latifolia* branches on  
208 different bushes. Each branch was measured over two sequential days: 8–9 Sep, 14–15 Sep,  
209 22–23 Sep, 12–13 Oct, 19–20 Oct, and 26–27 Oct. The bushes were at least 20 m apart, to  
210 enable selective irrigation for individual shrubs. Meteorological parameters were measured  
211 at a distance of 300–600 m from the branch measurements. These parameters included T  
212 and RH, measured using a Campbell HC2S3 probe; net radiation, measured with a CNR4  
213 Kipp & Zonen net radiometer; and wind speed and direction, recorded by a 05103 R.M.  
214 Young sensor. Eight 30-min samplings were performed per measurement day. In addition,  
215 two reference samplings were performed with full equipment setup, but no branch inside  
216 the bag. These reference samplings were performed before and after the eight  
217 measurements. On each measurement day, after completing the first sampling for reference,  
218 the system and branches were given at least 60 minutes to adapt to the different conditions

219 after placing the branch into the bag and setting up the equipment. At the end of the first  
220 measurement day, the sampled branch was removed from the bag and returned after the  
221 reference sampling on the second day. Following the 9<sup>th</sup> sampling on the second  
222 measurement day of each two-sequential-day period, the sampled branch was cut and sent  
223 to the laboratory for leaf analysis. Leaf wet weight and area were evaluated within 24 h  
224 after cutting the branch. All leaves were scanned, and a digital color-based image-  
225 processing method was used to identify the total (RGB values: 40–200, 50–200, 30–200)  
226 and healthy (RGB values: 40–110, 50–105, 30–80) leaf areas. The leaves were then dried  
227 for 72 h at 60 °C, and their net dry weight was recorded.

228 The sampling tubes were kept in a cooler with a temperature below 5 °C after the  
229 measurement, and analyzed within 5 days of sampling by GC–MS (see Sect. 2.3). Of the  
230 identified species, one MT and four SQT compounds (*cis*- $\beta$ -ocimene,  $\beta$ -caryophyllene,  $\alpha$ -  
231 humulene,  $\alpha$ -farnesene, and germacrene D) with the highest sampled mass for each of the  
232 branches were chosen for quantification by GC–MS (see Sect. 2.3).

233 The emission rate of BVOCs per leaf area,  $E_A$  (ng cm<sup>-2</sup> h<sup>-1</sup>), for a branch was  
234 evaluated by the following formula:

$$235 \quad E_A = \left( m \frac{F_{in-B}}{F_{out-T}} \right) / (A \cdot t) \quad (1)$$

236 where  $m$  (ng) is the evaluated mass of any BVOC compound inside the tube,  $F_{in-B}$  (L min<sup>-1</sup>)  
237 and  $F_{out-T}$  (mL min<sup>-1</sup>) are the flow rate pumped into the bag and the flow rate through  
238 the adsorbent tube, respectively,  $A$  (cm<sup>2</sup>) is the total leaf area of the branch, and  $t$  (h) is the  
239 sampling time.

240 The emission rate of BVOCs per biomass,  $E_M$  (ng g<sup>-2</sup> h<sup>-1</sup>), was evaluated by:

$$241 \quad E_M = \left( m \frac{F_{in-B}}{F_{out-T}} \right) / (M \cdot t) \quad (2)$$

242 where M (g) is the leaf biomass of the branch.

243

#### 244 **2.4.2 Irrigation and soil-water content quantification**

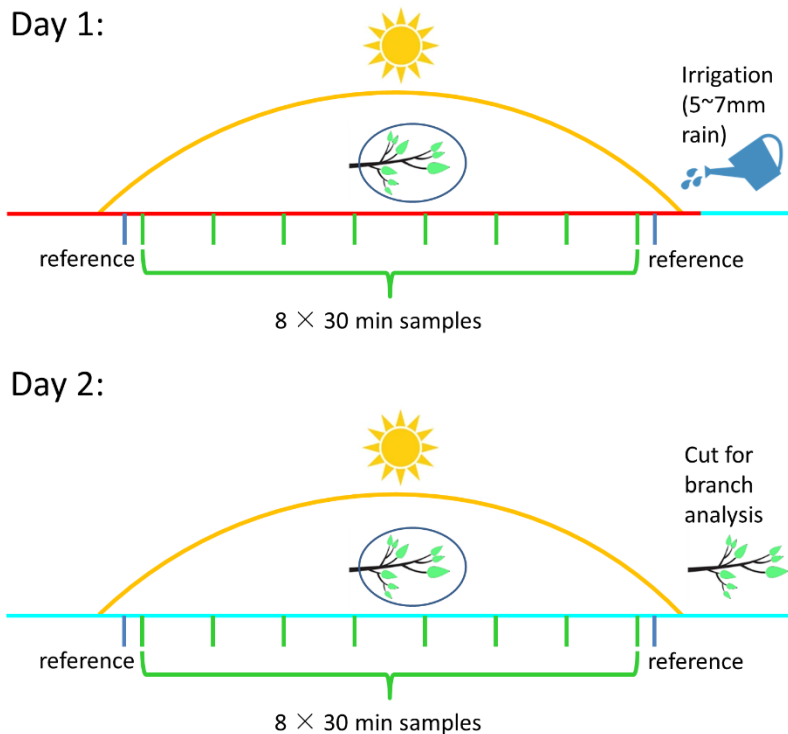
245 Manual irrigation was applied at the end of the first measurement day of each 2-sequential-

246 day measurement period (see Fig. 2). The irrigation amounts were 50–70 L within a radius

247 of 1–2 m from the stem of the plants used for sampling (equivalent to 5.5–7 mm rain). This

248 irrigation served to identify the potential effect of a small precipitation event during a

249 drought period on BVOC emission rate and composition.



250 **Figure 2.** Schematic of the experimental design. Day 1 and Day 2 represent, respectively, the first and

251 second day of each two-sequential-day sampling period for a specific branch. Green and blue bars represent

252 sampling measurements and reference measurements, respectively. The red and cyan lines mark sampling

253 prior to manual irrigation on Day 1 and after manual irrigation, on Day 2, respectively.

254 Ten soil samples were collected at solar noon time within 2 m from the sampled  
 255 plant on every experimental day. To evaluate the soil-water content, soil samples were  
 256 weighed on the day of collection, and weighed again after drying them in an oven at 105 °C  
 257 for 24 h. The following formula was used to calculate the soil-water content:

$$258 \quad w = \frac{M_{tot} - M_{dry}}{M_{dry}} \times 100\% \quad (3)$$

259 where  $w$  (g/g) is the soil gravimetric water content and  $M_{tot}$  (g) and  $M_{dry}$  (g) are the total  
 260 and dried soil mass, respectively.

261

### 262 ***2.4.3 Correlation between BVOC emission rate and temporal changes in RH and T***

263 To test the effect of instantaneous changes in RH and T on the emission rate of the sampled  
 264 BVOCs, we studied the correlation between the temporal changes in both ambient air RH  
 265 and T with the BVOC emission rate during the sampling. BVOC sampling length was 30  
 266 min, with a gap of 1 h between each sampling. To account for instantaneous changes in  
 267 RH and T we introduce  $\delta_{RH}$  and  $\delta_T$ , respectively.  $\delta_{RH}$  is defined as follows:

$$268 \quad \delta_{RH} = \sum_{i=1}^n \left( \frac{RH_{i+1}}{RH_i} - 1 \right) \quad (4)$$

269 where  $i$  is the 10 min time step according to the available measurement frequency, and  $n$   
 270 is the number of time steps.

271  $\delta_T$  is defined in the same manner as follows:

$$272 \quad \delta_T = \sum_{i=1}^n \left( \frac{T_{i+1}}{T_i} - 1 \right) \quad (5)$$

273 The correlations between  $\delta_{RH}$ ,  $\delta_T$  and the BVOC fluxes for all samples were tested  
 274 for different values of  $n$ . In a preliminary test, it was found that the highest average  
 275 correlations of  $\delta_{RH}$  and  $\delta_T$  with BVOC emission rate were obtained when  $n = 9$ .  
 276 Accordingly, the calculation duration of  $\delta_{RH}$  and  $\delta_T$  began 60 min before each 30 min

277 BVOC emission rate sampling. This finding is consistent with a similar analysis conducted  
278 by Li et al. (2024). Similarly, the correlation between  $\delta_{RH}$  and  $\delta_T$  and BVOC emission rate  
279 in that study applied  $\delta_{RH}$  and  $\delta_T$  which were calculated for 90 min cycles, while the  
280 beginning of each cycle was 60 min prior to the beginning of each compatible 30 min  
281 BVOC sampling.

282

#### 283 ***2.4.4 Afternoon emission trend (AET) analysis***

284 Under drought conditions, the increased stomatal resistance can largely reduce the BVOC  
285 emission rate (see Sect. 1). Accordingly, it was found that the BVOC mixing ratio tends to  
286 reach a minimum around noontime when RH tends to reach its daily minimum and stomatal  
287 conductance is limited (Nobel, 1999), and then gradually increase in the afternoon (Li et  
288 al., 2024). Our observations indicated a clear increase in BVOC emission rates during the  
289 afternoon for the days before the irrigation. On those days, no clear decrease in BVOC  
290 emission was observed before noon; instead, the BVOCs generally exhibited lower  
291 emission rates. Here we introduce a method for quantifying the trend of emission rate right  
292 after the mid-day minimum, which applies the afternoon emission trend (AET) index:

$$293 \quad \text{AET} = \sum_{i=1}^n \left( \frac{E_{i+1}}{E_i} - 1 \right) \quad (6)$$

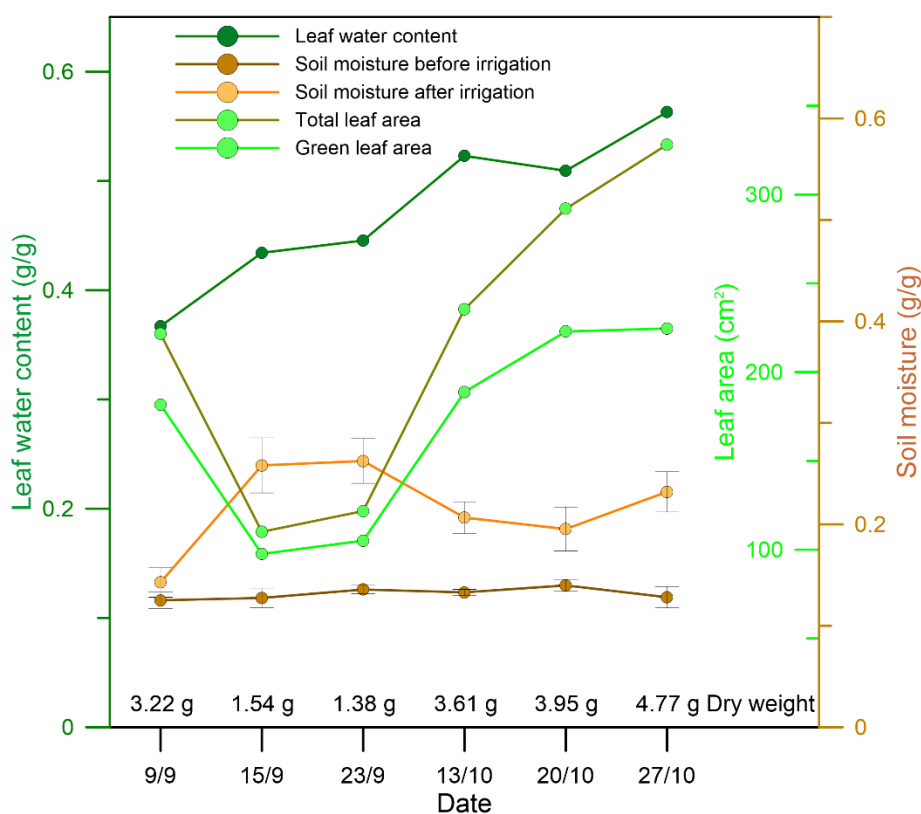
294 where  $E_i$  is the emission rate of the  $i_{\text{th}}$  sample, while  $i = 1$  indicates the minimum value  
295 around noontime, between 12:00–14:00 h. Hence, the AET indicates the trend and  
296 magnitude of the emission in the afternoon of any measurement day.

297 **3 Results and discussion**

298 **3.1 Analysis of branch leaves**

299 Figure 3 shows the total leaf area (cm<sup>2</sup>), green leaf area (cm<sup>2</sup>), leaf water content, and soil  
300 moisture before and after irrigation of each sampling branch. Leaf green area ranged from  
301 68% to 89% of the total leaf area. Soil moisture ranged from 12.5% to 14.0% before  
302 irrigation and from 14.3% to 26.2% after irrigation. Interestingly, the leaf water content  
303 after irrigation increased gradually during the experimental period, indicating that the  
304 capacity for water uptake from the soil increases with drought prolongation.

305



306 **Figure 3.** Properties of the sampled branch leaves and soil moisture within a radius of 1 m from the stem of  
307 the sampling plant. Presented leaf property values are averages over all sampled branch leaves.

## 308 **3.2 Emission rates of MTs and SQTs**

309 Whereas previous branch enclosure studies focused primarily on isoprene emissions  
310 (Genard-Zielinski et al., 2015; Genard-Zielinski et al., 2018; Saunier et al., 2017), our  
311 measurements did not detect large amounts of isoprene emissions from the selected  
312 *Phillyrea latifolia*, in line with previous studies showing that some plant types do not emit  
313 notable amounts of isoprene (Aydin et al., 2014; Bracho-Nunez et al., 2013). Our analysis  
314 focused on the MTs and SQTs detected in our observations, as described in the following  
315 section.

316

### 317 **3.2.1 MTs**

318 On all 10 sampling days for which MTs were identified, the 5 days prior to irrigation were  
319 under drought conditions (i.e., more than 100 days after the last precipitation event), and 5  
320 days were under irrigation conditions on the same branches (see Sect. 2.4.2). The branch  
321 which was sampled on Sep 14–15 did not show any detectable MT emission. The diurnal  
322 emission fluxes of MTs from the branches are shown in Fig. 4.

323 The daily average emission rate of MTs over all sampling days ranged from 11.7–  
324 2151.4 ng cm<sup>-2</sup> h<sup>-1</sup> (0.89–121.5 μg g<sup>-1</sup> h<sup>-1</sup>), with *cis*-β-ocimene being the most abundant for  
325 each of the sampling branches, averaging at 88% of all detected MTs. These MT emission  
326 rates are similar to previous branch enclosure studies, which were conducted  
327 predominantly between May and October under Western Mediterranean conditions, where  
328 they ranged from 0 to approximately 140 μg g<sup>-1</sup> h<sup>-1</sup> (Bracho-Nunez et al., 2013; Llusia and  
329 Peñuelas, 2000; Núñez et al., 2002; Owen et al., 1997; Owen and Hewitt, 2000; Staudt et  
330 al., 2001; Street et al., 1997). Less information is available on the emission rates of MTs in

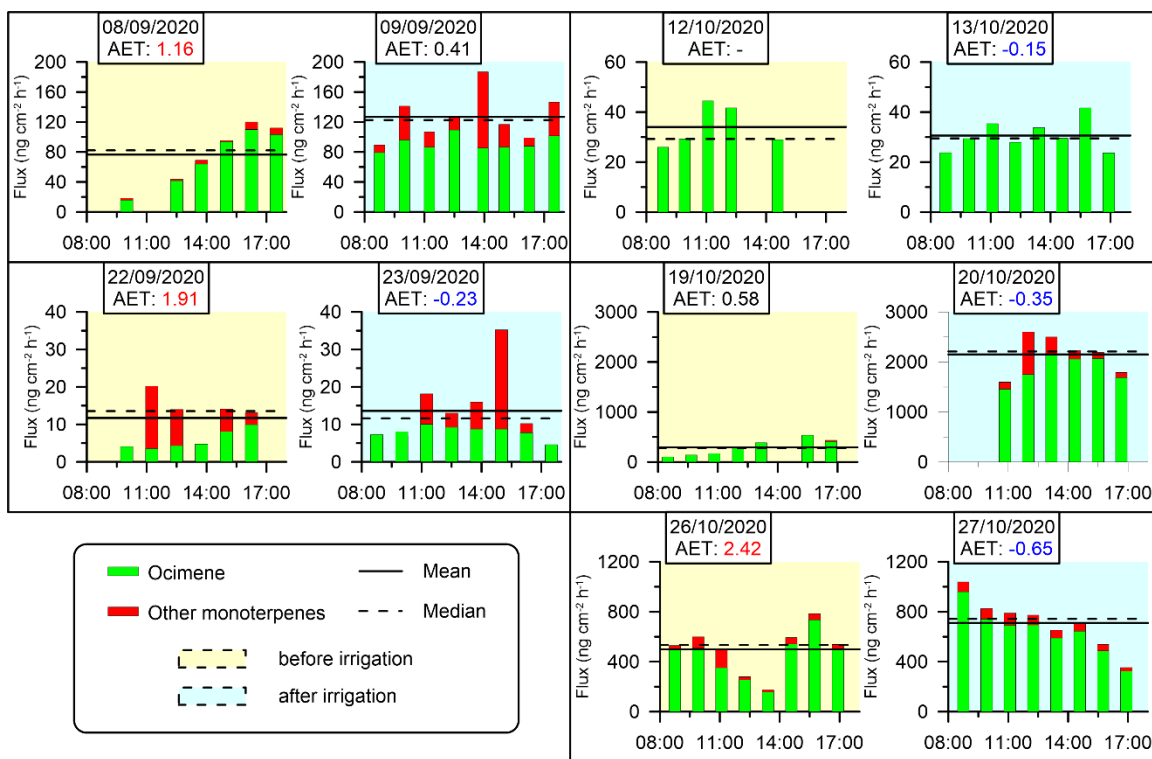


331 the Eastern Mediterranean. Aydin et al. (2014) used a branch enclosure system to detect  
332 emission rates ranging from 0.0047 to 14.2  $\mu\text{g g}^{-1} \text{h}^{-1}$  in 14 different forested areas in  
333 Turkey. Seco et al. (2017) quantified MT emissions using eddy covariance method in pine  
334 forests in Israel, studying a semiarid site (Yatir) and a Mediterranean sub-humid site (Birya)  
335 in the spring. Emission fluxes were found to average at 40  $\text{ng cm}^{-2} \text{h}^{-1}$  (Yatir) and 100  $\text{ng}$   
336  $\text{cm}^{-2} \text{h}^{-1}$  (Birya), with peak values of 100 (Yatir) and 190 (Birya)  $\text{ng cm}^{-2} \text{h}^{-1}$ , while the  
337 daytime standardized MT emission capacities were similar across both sites.

338 In our study, MT emissions under drought conditions ranged from 11.7  $\text{ng cm}^{-2} \text{h}^{-1}$   
339 to 499.0  $\text{ng cm}^{-2} \text{h}^{-1}$ , which is somewhat higher than other values reported in the Eastern  
340 Mediterranean. It is important to note that differences in emission rates between our study  
341 and the previously reported values in this region might be attributed to the different  
342 measurement methodologies employed. Following irrigation, the mean daily MT emission  
343 rates increased in four out of the five investigated branches, and ranged from 13.6  $\text{ng cm}^{-2}$   
344  $\text{h}^{-1}$  to 2151.4  $\text{ng cm}^{-2} \text{h}^{-1}$ . This reflects an average 150% increase for all sampling days in  
345 the range of emission rates following irrigation, indicating that even a small amount of  
346 water during a period of drought stress can significantly influence MT emissions. This  
347 effect may be related to the dramatic increase in stomatal conductance, due to the increase  
348 in water availability following irrigation (Medrano et al., 2002; Miyashita et al., 2005;  
349 Vilagrosa et al., 2003). It is also observed that on some of the sampling days, the  
350 composition of MTs tends to become more diverse after irrigation compared to before  
351 irrigation, warranting further study.

352 AET (Sect. 2.4.4) values specified in figures 4 and 5 reinforced the significant effect of  
353 small irrigation amounts on BVOC emission rates under drought, considering that on

354 drought days, AETs were high and positive, whereas after irrigation, AETs became  
 355 moderate or negative. This observation is consistent with previous studies showing that the  
 356 emission of BVOCs can be affected by the vegetation's stomatal activity, which tends to  
 357 be lower around noontime during drought stress (Li et al., 2023; Seco et al., 2017). Stomatal  
 358 resistance is typically two orders of magnitude larger than cuticular resistance (Nobel, 1999)  
 359 and therefore, the midday minimum and the following increase in MT emissions under  
 360 drought conditions may be mostly due to stomatal resistance, which can limit the exchange  
 361 of gases between the plant and the atmosphere. In other words, the increased emission of  
 362 MTs after irrigation may be due to reopening of the stomata, which allows for the release  
 363 of VOCs.



364 **Figure. 4** Branches' diurnal MT emission fluxes. No MTs were detected for the branch sampled on 14–15  
 365 Sep. Yellow and blue shading indicate the days before and after irrigation, respectively (see Sect. 2.4.2).  
 366 Horizontal solid and dashed lines are daytime mean and median fluxes of MTs, respectively. AET values  
 367 (see Sect. 2.4.4) are marked in red and blue when they are larger than 1 or negative, respectively.

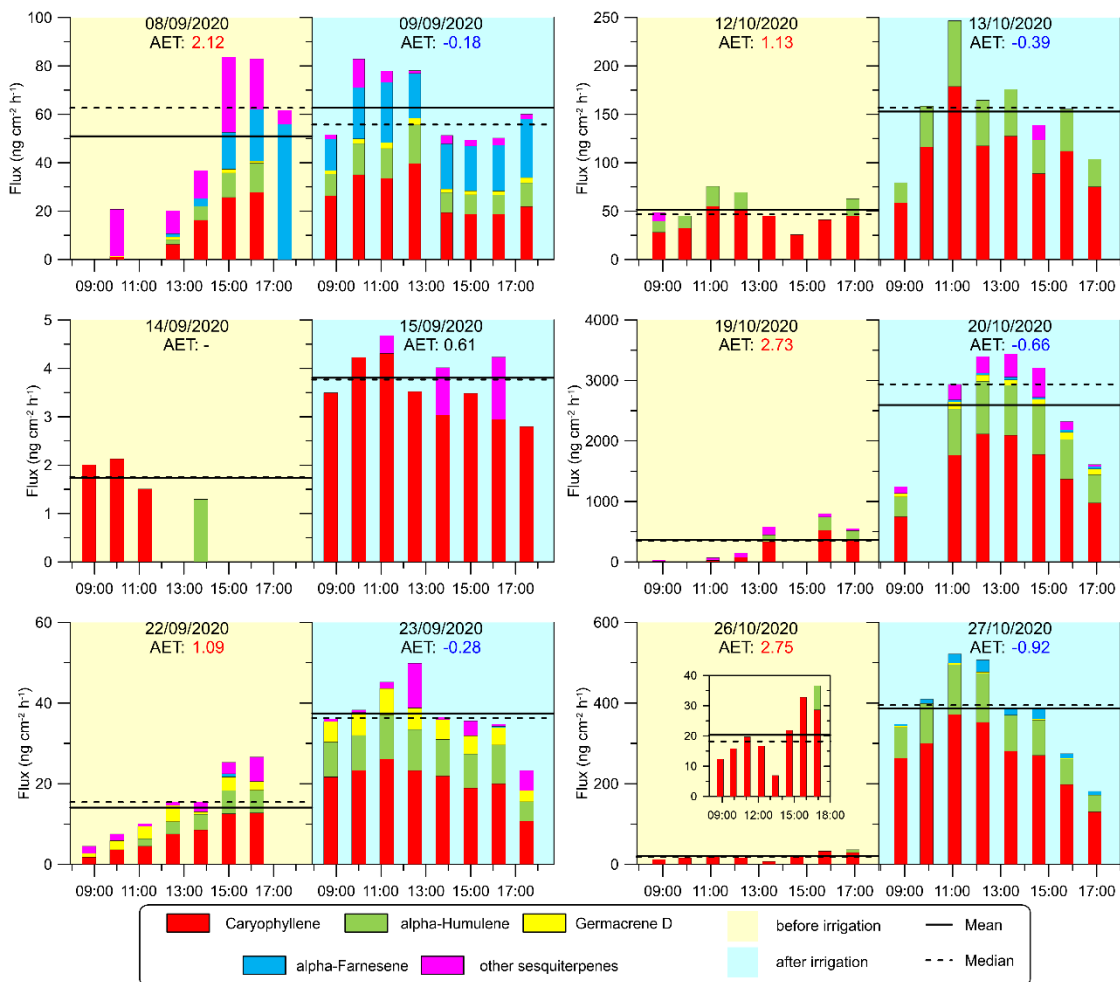
### 368 3.2.2 SQTs

369 Figure 5 shows the emission fluxes of SQTs for the branches under drought and irrigation  
370 conditions. The four most abundant detected SQTs for each of the sampled branches were  
371  $\beta$ -caryophyllene,  $\alpha$ -humulene, germacrene D, and  $\alpha$ -farnesene. These compounds  
372 comprised 90% of all detected SQTs, from all the branches together. The daily average  
373 emission rate of SQTs ranged from 1.7–2595.7 ng cm<sup>-2</sup> h<sup>-1</sup> (0.11–146.6  $\mu$ g g<sup>-1</sup> h<sup>-1</sup>). In  
374 contrast to MTs, few studies provide branch enclosure measurements for SQTs. Notably,  
375 our study found significantly higher emission rates than previous research conducted  
376 between June and October under Eastern Mediterranean conditions, where rates ranged  
377 from 0.0011 to 0.63  $\mu$ g g<sup>-1</sup> h<sup>-1</sup> (Aydin et al., 2014; Bracho-Nunez et al., 2013). The emission  
378 fluxes of the SQTs were overall comparable to those of the MTs, which is a notable finding,  
379 considering that SQT emission rates are frequently around a quarter of the MT flux  
380 (Saunders et al., 2003; Sindelarova et al., 2014). The finding of relatively high SQT  
381 emission rates appears to be in line with the findings of Li et al. (2023), who reported  
382 relatively high mixing ratios of SQTs (33.6 times higher than isoprene, and 18.9 times  
383 higher than MTs) under drought conditions in the same region.

384 Furthermore, we found that the increase in SQT emission flux following irrigation  
385 (by 545% on average) was more significant than that of the MTs (by 150% on average).  
386 This suggests that the response of SQT emissions to water availability is stronger than that  
387 of MTs, which could be related to the chemical properties and physiological functions of  
388 SQTs in plants. Bonn et al. (2019) found that a sharp increase in SQT emission occurs  
389 close to the wilting point to protect the plant against oxidative damage, as also supported  
390 by Caser et al. (2019). The latter found that drought can induce the SQT-synthesis

391 mechanism. The strong increase in SQT emission after irrigation in our study further  
 392 supports the notion that enhanced synthesis of SQTs occurs shortly after the release of  
 393 drought stress. In addition, the SQTs composition, like MTs composition, was observed to  
 394 be more diverse after irrigation in most cases, warranting further study.

395



396 **Figure. 5** Diurnal SQT emission fluxes from the sampled branches. Column colors represent the emission  
 397 fluxes of four types of SQTs, and the magenta section of the columns refers to other SQTs. Yellow and  
 398 blue shading indicate the days before and after irrigation, respectively (see Sect. 2.4.2). Horizontal solid  
 399 and dashed lines are daytime mean and median SQT flux rates, respectively. AET values (see Sect. 2.4.4)  
 400 are marked in red and blue when they are larger than 1 or negative, respectively. To better present the trend  
 401 on 26 Oct, a smaller figure with a smaller scale is added.

402 Interestingly, the high SQT emission rates found in this study are consistent with  
403 the findings of a previous study conducted in the same area (Li et. al., 2023), which also  
404 reported higher emission fluxes of SQTs compared to other studies. This suggests that there  
405 may be a unique level of drought or plant characteristics that contribute to the high emission  
406 fluxes of SQTs in this region.

407

### 408 *3.3 The impact of meteorological parameters on MT and SQT emission rates under* 409 *drought condition*

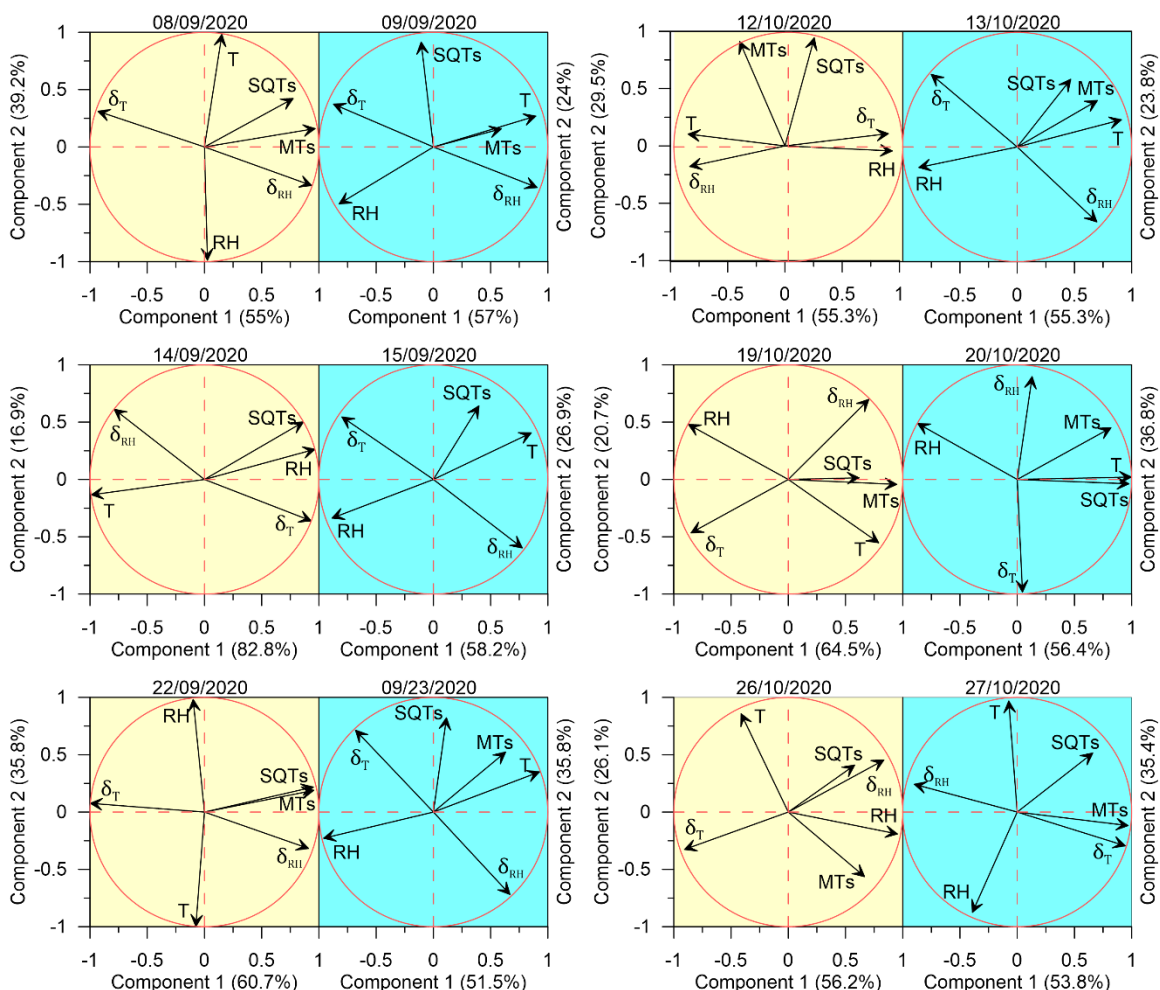
410 The effect of meteorological conditions on BVOC emission rate under drought conditions  
411 is complex and depends on many factors, including vegetation type, BVOC type, and  
412 ambient stress. In the Eastern Mediterranean region, Li et al. (2023) found that under  
413 drought, the best proxy for BVOC emission is the instantaneous temporal change in RH;  
414 temporal changes in T were also better correlated with BVOC mixing ratio than absolute  
415 values of T. Here, we examined the impact of instantaneous changes in ambient air RH and  
416  $T - \delta_{RH}$  and  $\delta_T$ , respectively (see Sect. 2.4.3), as well as of ambient air T and RH on the  
417 BVOC emission rate. Due to the large variation in BVOC emissions across different  
418 branches, the r values were calculated separately for each branch and each sampling day.  
419 Figure 6 presents a principal component analysis (PCA) for the correlation of both  $\delta_{RH}$  and  
420  $\delta_T$  with the BVOC emission rates. Before irrigation, when the plants were under drought,  
421 on 8 Sep, 22 Sep, 19 Oct, and 26 Oct, the emission rates of the measured BVOC (including  
422 both MTs and SQTs) were better correlated with  $\delta_{RH}$  and  $\delta_T$  (average Pearson's value (r)  
423 of 0.56 and -0.61, respectively) than with RH and T (r of -0.22 and 0.29, respectively).  
424 Exceptional are 14 Sep and 12 Oct, also sampled under drought conditions: on 14 Sep, the

425 SQT emissions showed the best correlation with RH ( $r = 0.97$ ); on 12 Oct, the emission  
426 rates of BVOCs tended not to correlate with any of the tested meteorological parameters  
427 because of a strong correlation of T and  $\delta_{RH}$  ( $r = -0.98$ ).

428         When focusing only on the days after irrigation, except for 27 Oct, the BVOC  
429 emissions were better correlated with T (averaging  $r$  values across all relevant days,  $r =$   
430  $0.52$ ) than with any other parameter. Interestingly, on 27 Oct, the SQTs tended to correlate  
431 with RH ( $-0.58$ ), while the MT emission was better correlated with  $\delta_T$  ( $0.94$ ). The PCA  
432 results show some similarities between the different sampled branches, in their stronger  
433 response to  $\delta_{RH}$  than to the other tested meteorological parameters and their almost  
434 complete lack of correlation with T when under drought conditions. However, after  
435 irrigation, all BVOC emission rates were highly responsive to T, more than to any other  
436 parameter, reflecting the well-known Arrhenius-type increase for BVOC emission with  
437 temperature, as mentioned in Sect. 1.

438         Table 1 summarizes the correlation coefficients between the emission rates of  
439 SQTs/MTs and RH, T,  $\delta_{RH}$ , and  $\delta_T$ , both before and after irrigation. Considering the  
440 significant variability in the emission rates of SQTs and MTs across different branches, the  
441  $r$  values presented in the table are averages calculated from individual branch-level  $r$  values,  
442 separately before and after irrigation. Li et al. (2023) showed that under drought conditions,  
443 the temporal gradient of meteorological parameters in general was more strongly correlated  
444 with BVOC emission rates – not only for RH, but also for T and vapor-pressure deficit.  
445 Before irrigation, both SQT and MT emission rates were more strongly correlated with  $\delta_{RH}$

446 and  $\delta_T$  than with RH and T. However, after irrigation, the r values for the correlations with  
 447  $\delta_{RH}$  and  $\delta_T$  were dramatically weakened. Moreover, following irrigation, the correlations



448 **Figure. 6** PCA analysis for the response of SQTs and MTs to meteorological parameters. The results are

449 presented for SQTs, MTs, T, RH,  $\delta_T$ , and  $\delta_{RH}$ , individually for each measurement day. The yellow and  
 450 blue shaded areas refer to the day before and after irrigation, respectively.

451

452 with T and RH for both MTs and SQTs were notably stronger than before the irrigation.

453 This indicates that under drought, the temporal gradients in T and RH have a stronger

454 impact on BVOC emissions than the absolute value of T and RH, in agreement with

455 findings by Li et al. (2023). Here, we demonstrate that even a relatively minor precipitation

456 event leads to T becoming the dominant factor in the BVOC emission rate, as expected

457 under non-drought conditions. Interestingly, after irrigation, the highest  $r$  value for MTs  
 458 was with T, but for SQTs, it was with RH.

459

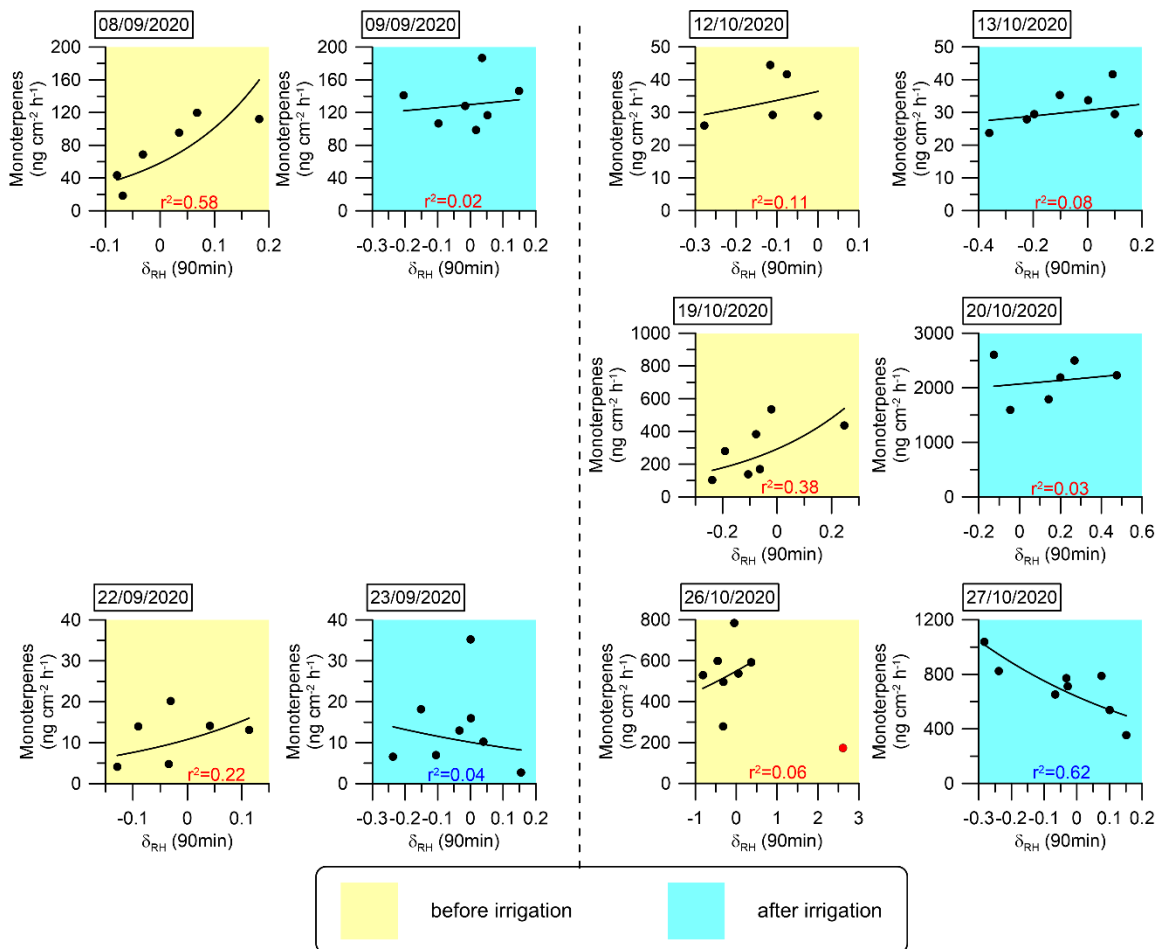
460 **Table 1.** Correlation between the emission rates of MTs and SQTs and the examined meteorological  
 461 parameters. Presented are the Pearson's  $r$  values for the correlation between MT/SQT emission rate and RH,  
 462 T,  $\delta_{RH}$ , and  $\delta_T$  (green shading for SQT emissions and lavender shading for MT emissions). The values are  
 463 the average of  $r$  values across multiple individual branches. Blue and red shading indicates positive and  
 464 negative correlation, respectively, and the darkness of the color indicates their values. The  $P$ -values for the  
 465 correlation are shown in brackets.

Pearson's $r$ value					
SQT	before irrigation	after irrigation	MT	before irrigation	after irrigation
vs RH	-0.22 (0.00)	-0.46 (0.00)	vs RH	-0.18 (0.11)	-0.44 (0.04)
vs T	0.33 (0.02)	0.42 (0.00)	vs T	0.20 (0.02)	0.46 (0.01)
vs $\delta_{RH}$	0.53 (0.02)	-0.11 (0.00)	vs $\delta_{RH}$	0.54 (0.01)	0.00 (0.00)
vs $\delta_T$	-0.50 (0.02)	0.13 (0.00)	vs $\delta_T$	-0.48 (0.01)	0.03 (0.00)

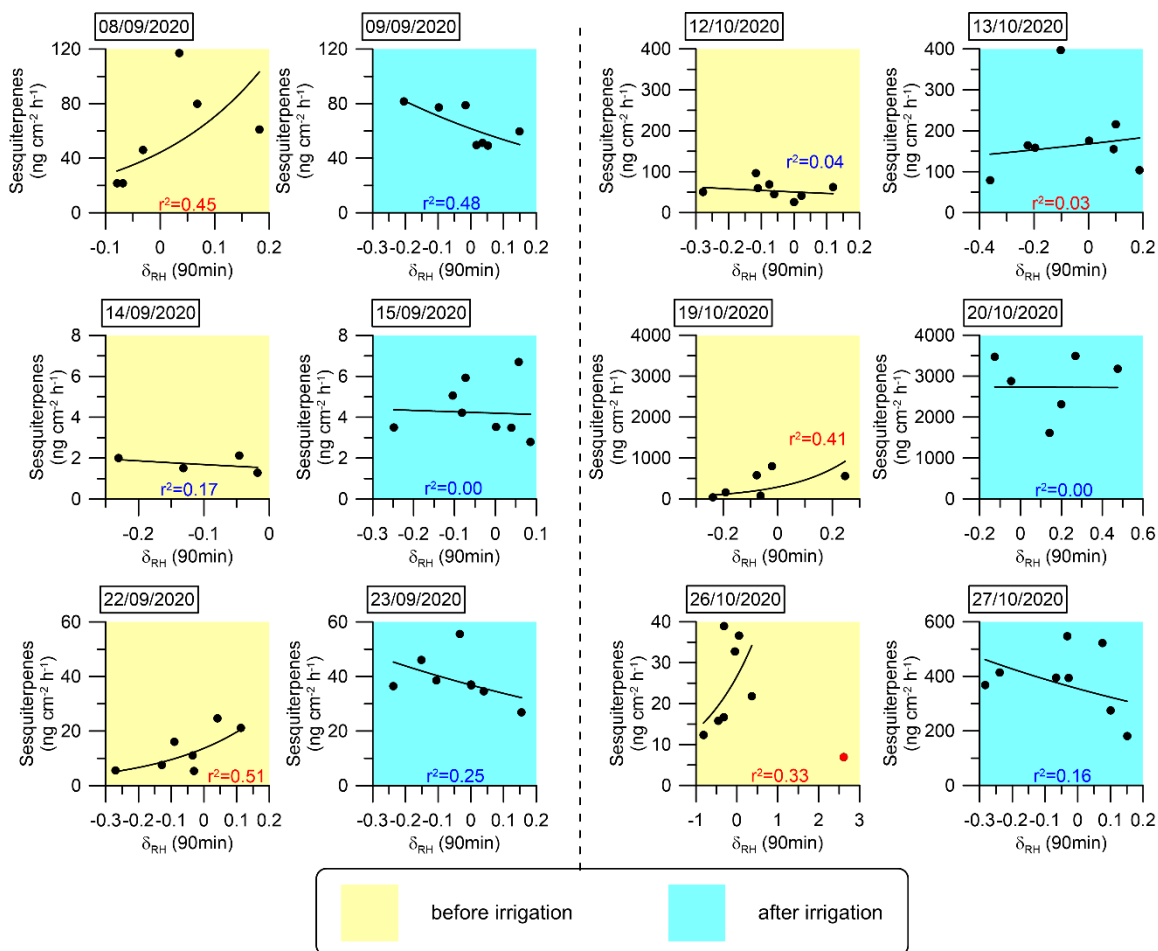
466 The analysis presented in Fig. 6 and Table 1 reinforces the finding that  
 467 instantaneous changes in meteorological parameters, particularly  $\delta_{RH}$ , serve as a better  
 468 proxy for BVOC emission rate under drought conditions. This finding suggests that  
 469 modeling BVOC emission rates under drought conditions can rely on  $\delta_{RH}$ . In light of this  
 470 insight, we investigated the mathematical connection between  $\delta_{RH}$  and the emission rates  
 471 of the MT and SQT fluxes. Exponential fitting corresponded with a relatively strong  
 472 correlation between these emission rates and  $\delta_{RH}$ . Other fitting types used to test this  
 473 relationship are presented in Sect. S2. Figures 7 and 8 depict the exponential fitting curves  
 474 for MTs and SQTs, respectively. These curves are presented separately for each branch



475 and individually for drought and post-irrigation conditions. The  $r^2$  for MTs with  $\delta_{RH}$  ranged  
 476 from 0.06 to 0.58 ( $r = 0.24$ – $0.76$ , average 0.48) under drought, whereas following irrigation,  
 477 the corresponding correlations ranged from 0.02 to 0.62 ( $r = -0.78$ – $0.28$ , average  $-0.08$ ).  
 478 For SQTs, the corresponding  $r^2$  values were somewhat higher, ranging from 0.04 to 0.51 ( $r$   
 479 =  $-0.41$ – $0.67$ , average  $+0.33$ ) and 0.00 to 0.48 ( $r = -0.69$ – $0.17$ , average  $-0.24$ ), under  
 480 drought and following irrigation, respectively.



481 **Figure. 7** Daily correlations between MT emission fluxes and  $\delta_{RH}$ . An exponential fitting function was used  
 482 to fit the curves. The coefficient of determination ( $r^2$ ) for each day is marked in red or blue when the  
 483 correlation is positive or negative, respectively.



484 **Figure. 8** Daily correlations between SQT emission fluxes and  $\delta_{RH}$ . An exponential fitting function was  
 485 used to fit the curves. The coefficient of determination ( $r^2$ ) for each day is marked in red or blue when the  
 486 correlation is positive or negative, respectively. The sample at 12:10 h on 26 Oct 2020 (marked in red) was  
 487 not considered in the fitting curve for that day, because an extremely sharp increase in RH (from 10 to 31%)  
 488 occurred within 10 min, which we considered an outlier.

489  
 490 Overall, these results suggest that while  $\delta_{RH}$  is likely a better proxy for MT and  
 491 SQT emission rates (see Table 1 and Sect. S3), the correlation of  $\delta_{RH}$  with these BVOCs  
 492 appears to be too weak to accurately predict their emission rates using  $\delta_{RH}$  values in  
 493 atmospheric modeling. Additional study is needed before  $\delta_{RH}$  can effectively serve as a  
 494 parameter for modeling BVOC emission rates.

495           Following irrigation, the correlations between the emission flux rates and  $\delta_{RH}$   
496 became more moderate (4 cases out of 11) or even negative (5 cases out of 11). This further  
497 demonstrates the high sensitivity of  $\delta_{RH}$ 's effect on BVOC emissions to changes in water  
498 availability. Further research is required to examine the physiological and biochemical  
499 processes underlying the sensitivity of BVOC emission rates to  $\delta_{RH}$ .

500

#### 501 **4 Summary and conclusions**

502 We investigated BVOC emission rates from branches of *Phillyrea latifolia* under both  
503 drought and minor irrigation conditions in the Eastern Mediterranean region, with the aim  
504 of assessing the influence of low precipitation levels and meteorological parameters on MT  
505 and SQT emission rates during drought stress. We found that leaf water content increases  
506 gradually under prolonged periods of drought, indicating the plant's enhanced capacity for  
507 water uptake under more severe drought conditions. The highest emission rate among all  
508 detected MTs was of *cis*- $\beta$ -ocimene, and among the detected SQTs,  $\beta$ -caryophyllene,  $\alpha$ -  
509 humulene, germacrene D, and  $\alpha$ -farnesene. Both the MT and SQT emission rates were  
510 significantly influenced by the availability of soil water. In response to irrigation, the MT  
511 and SQT emission rates increased by 150% and 545%, respectively, indicating that even a  
512 small amount of water (equivalent to 5.5–7 mm precipitation) can significantly impact their  
513 emission rates.

514           This study highlights the complex way in which meteorological conditions affect  
515 BVOC emissions under drought conditions. In line with Li et al.'s (2023) findings, under  
516 drought, the instantaneous change of relative humidity,  $\delta_{RH}$  was the best proxy for BVOC  
517 emission rates, as its correlation with MTs and SQTs emission rate ( $r = 0.54$  and  $0.53$ ,  
518 respectively) was the strongest among all tested meteorological parameters. However, after

519 a small amount of irrigation (equivalent to 5.5–7 mm precipitation), no correlation was  
520 observed between  $\delta_{RH}$  and MT emission rate, whereas a negative correlation with  $\delta_{RH}$  was  
521 observed for SQT emission rate. The increase in soil water availability led to T (for MTs)  
522 or RH (for SQTs) becoming the dominant meteorological parameter affecting BVOC  
523 emission rate, making them the best proxies for BVOC emission rates among all tested  
524 meteorological parameters. This indicates that changes in water availability can  
525 dramatically alter the manner in which BVOC emissions respond to meteorological  
526 conditions.

527         Hence, according to the conditions used in this study, under more severe drought,  
528  $\delta_{RH}$  can serve as the best proxy for BVOC emission rate, whereas under more moderate  
529 drought, either T or RH is the best proxy for BVOCs, in agreement with previous findings  
530 presented in the companion paper by (Li et al., 2023). Our findings indicate that even a  
531 small amount of precipitation can lead to a transition from a drought to non-drought regime  
532 in terms of BVOC emission rates and the manner in which they respond to meteorological  
533 conditions.

534

535 **Author contribution.** ET designed the experiments, QL and GL carried out the field  
536 measurements, QL performed the data acquisition. QL performed the analytical analysis  
537 together with EB and EL. QL and ET led the data analyses with contributions from all co-  
538 authors. QL and ET prepared the manuscript with contributions from EB.

539

540 **Competing interests.** The authors declare that they have no conflict of interest.

541 **Acknowledgements**

542 This study was supported by the Israel Science Foundation, Grant Nos. 1787/15 and  
543 543/22. Eran Tas holds the Joseph H. and Belle R. Braun Senior Lectureship in Agriculture.

544

545 **References**

- 546 Asensio D., Peñuelas J., Llusià J., Ogaya R., Filella I., 2007. Interannual and interseasonal soil CO<sub>2</sub>  
547 efflux and VOC exchange rates in a Mediterranean holm oak forest in response to  
548 experimental drought. *Soil Biology and Biochemistry* 39(10),2471–2484.  
549 <https://doi.org/10.1016/j.soilbio.2007.04.019>.
- 550 Aydin Y.M., Yaman B., Koca H., Dasdemir O., Kara M., Altioek H., Dumanoglu Y., Bayram A., Tolunay  
551 D., Odabasi M., Elbir T., 2014. Biogenic volatile organic compound (BVOC) emissions from  
552 forested areas in Turkey: Determination of specific emission rates for thirty-one tree species.  
553 *The Science of the total environment* 490,239–253.  
554 <https://doi.org/10.1016/j.scitotenv.2014.04.132>.
- 555 Baldwin I.T., Halitschke R., Paschold A., Dahl C.C. von, Preston C.A., 2006. Volatile signaling in  
556 plant-plant interactions: "talking trees" in the genomics era. *Science (New York, N.Y.)*  
557 311(5762),812–815. <https://doi.org/10.1126/science.1118446>.
- 558 Berg A.R., Heald C.L., Huff Hartz K.E., Hallar A.G., Meddens A.J.H., Hicke J.A., Lamarque J.-F., Tilmes  
559 S., 2013. The impact of bark beetle infestations on monoterpene emissions and secondary  
560 organic aerosol formation in western North America. *Atmos. Chem. Phys.* 13(6),3149–3161.  
561 <https://doi.org/10.5194/acp-13-3149-2013>.
- 562 Blande J.D., Tiiva P., OKSANEN E., Holopainen J.K., 2007. Emission of herbivore-induced volatile  
563 terpenoids from two hybrid aspen (*Populus tremula* × *tremuloides*) clones under ambient and  
564 elevated ozone concentrations in the field. *Glob Change Biol* 13(12),2538–2550.  
565 <https://doi.org/10.1111/j.1365-2486.2007.01453.x>.
- 566 Bonn B., Magh R.-K., Rombach J., Kreuzwieser J., 2019. Biogenic isoprenoid emissions under  
567 drought stress: Different responses for isoprene and terpenes. *Biogeosciences* 16(23),4627–  
568 4645. <https://doi.org/10.5194/bg-16-4627-2019>.
- 569 Bracho-Nunez A., Knothe N.M., Welter S., Staudt M., Costa W.R., Liberato M.A.R., Piedade M.T.F.,  
570 Kesselmeier J., 2013. Leaf level emissions of volatile organic compounds (VOC) from some  
571 Amazonian and Mediterranean plants. *Biogeosciences* 10(9),5855–5873.  
572 <https://doi.org/10.5194/bg-10-5855-2013>.
- 573 Brilli F., Barta C., Fortunati A., Lerdau M., Loreto F., Centritto M., 2007. Response of isoprene  
574 emission and carbon metabolism to drought in white poplar (*Populus alba*) saplings. *New  
575 Phytol* 175(2),244–254. <https://doi.org/10.1111/j.1469-8137.2007.02094.x>.
- 576 Brilli F., Ciccioli P., Frattoni M., Prestinini M., Spanedda A.F., Loreto F., 2009. Constitutive and  
577 herbivore-induced monoterpenes emitted by *Populus x euroamericana* leaves are key

578 volatiles that orient *Chrysomela populi* beetles. *Plant, cell & environment* 32(5),542–552.  
579 <https://doi.org/10.1111/j.1365-3040.2009.01948.x>.

580 Cai M., An C., Guy C., 2021. A scientometric analysis and review of biogenic volatile organic  
581 compound emissions: Research hotspots, new frontiers, and environmental implications.  
582 *Renewable and Sustainable Energy Reviews* 149(13),111317.  
583 <https://doi.org/10.1016/j.rser.2021.111317>.

584 Calfapietra C., Fares S., Manes F., Morani A., Sgrigna G., Loreto F., 2013. Role of Biogenic Volatile  
585 Organic Compounds (BVOC) emitted by urban trees on ozone concentration in cities: A review.  
586 *Environmental pollution (Barking, Essex 1987)* 183,71–80.  
587 <https://doi.org/10.1016/j.envpol.2013.03.012>.

588 Caser M., Chitarra W., D'Angiolillo F., Perrone I., Demasi S., Lovisolo C., Pistelli L., Pistelli L., Scariot  
589 V., 2019. Drought stress adaptation modulates plant secondary metabolite production in  
590 *Salvia dolomitica* Codd. *Industrial Crops and Products* 129,85–96.  
591 <https://doi.org/10.1016/j.indcrop.2018.11.068>.

592 Curci G., Beekmann M., Vautard R., Smiątek G., Steinbrecher R., Theloke J., Friedrich R., 2009.  
593 Modelling study of the impact of isoprene and terpene biogenic emissions on European ozone  
594 levels. *Atmospheric Environment* 43(7),1444–1455.  
595 <https://doi.org/10.1016/j.atmosenv.2008.02.070>.

596 Dayan C., Fredj E., Misztal P.K., Gabay M., Guenther A.B., Tas E., 2020. Emission of biogenic volatile  
597 organic compounds from warm and oligotrophic seawater in the Eastern Mediterranean.  
598 *Atmos. Chem. Phys.* 20(21),12741–12759. <https://doi.org/10.5194/acp-20-12741-2020>.

599 Duhl T.R., Helmig D., Guenther A., 2008. Sesquiterpene emissions from vegetation: A review.  
600 *Biogeosciences* 5(3),761–777. <https://doi.org/10.5194/bg-5-761-2008>.

601 Filella I., Primante C., Llusà J., Martín González A.M., Seco R., Farré-Armengol G., Rodrigo A.,  
602 Bosch J., Peñuelas J., 2013. Floral advertisement scent in a changing plant-pollinators market.  
603 *Scientific reports* 3,3434. <https://doi.org/10.1038/srep03434>.

604 Fitzky A.C., Kaser L., Peron A., Karl T., Graus M., Tholen D., Halbwirth H., Trimmel H., Pesendorfer  
605 M., Rewald B., Sandén H., 2023. Same, same, but different: Drought and salinity affect BVOC  
606 emission rate and alter blend composition of urban trees. *Urban Forestry & Urban Greening*  
607 80(7),127842. <https://doi.org/10.1016/j.ufug.2023.127842>.

608 Fortunati A., Barta C., Brilli F., Centritto M., Zimmer I., Schnitzler J.-P., Loreto F., 2008. Isoprene  
609 emission is not temperature-dependent during and after severe drought-stress: A  
610 physiological and biochemical analysis. *The Plant journal for cell and molecular biology*  
611 55(4),687–697. <https://doi.org/10.1111/j.1365-313X.2008.03538.x>.

612 Genard-Zielinski A.-C., Boissard C., Fernandez C., Kalogridis C., Lathière J., Gros V., Bonnaire N.,  
613 Ormeño E., 2015. Variability of BVOC emissions from a Mediterranean mixed forest in  
614 southern France with a focus on *Quercus pubescens*. *Atmos. Chem. Phys.*  
615 15(1),431–446. <https://doi.org/10.5194/acp-15-431-2015>.

616 Genard-Zielinski A.-C., Boissard C., Ormeño E., Lathière J., Reiter I.M., Wortham H., Orts J.-P.,  
617 Temime-Roussel B., Guenet B., Bartsch S., Gauquelin T., Fernandez C., 2018. Seasonal  
618 variations of *Quercus pubescens*; isoprene emissions from an *in*  
619 *natura* forest under drought stress and sensitivity to future climate change in the

620 Mediterranean area. *Biogeosciences* 15(15),4711–4730. [https://doi.org/10.5194/bg-15-](https://doi.org/10.5194/bg-15-4711-2018)  
621 4711-2018.

622 Geron C., Daly R., Harley P., Rasmussen R., Seco R., Guenther A., Karl T., Gu L., 2016. Large  
623 drought-induced variations in oak leaf volatile organic compound emissions during PINOT  
624 NOIR 2012. *Chemosphere* 146,8–21. <https://doi.org/10.1016/j.chemosphere.2015.11.086>.

625 Giorgi F., Lionello P., 2008. Climate change projections for the Mediterranean region. *Global and*  
626 *Planetary Change* 63(2-3),90–104. <https://doi.org/10.1016/j.gloplacha.2007.09.005>.

627 Goldstein A.H., McKay M., Kurpius M.R., Schade G.W., Lee A., Holzinger R., Rasmussen R.A., 2004.  
628 Forest thinning experiment confirms ozone deposition to forest canopy is dominated by  
629 reaction with biogenic VOCs. *Geophys. Res. Lett.* 31(22),22,123.  
630 <https://doi.org/10.1029/2004GL021259>.

631 Greenberg J.P., Asensio D., Turnipseed A., Guenther A.B., Karl T., Gochis D., 2012. Contribution of  
632 leaf and needle litter to whole ecosystem BVOC fluxes. *Atmospheric Environment* 59,302–311.  
633 <https://doi.org/10.1016/j.atmosenv.2012.04.038>.

634 Guenther A., 2013. Biological and Chemical Diversity of Biogenic Volatile Organic Emissions into  
635 the Atmosphere. *ISRN Atmospheric Sciences* 2013(19),1–27.  
636 <https://doi.org/10.1155/2013/786290>.

637 Guenther A., Hewitt C.N., Erickson D., Fall R., Geron C., Graedel T., Harley P., Klinger L., Lerdau M.,  
638 McKay W.A., Pierce T., Scholes B., Steinbrecher R., Tallamraju R., Taylor J., Zimmerman P.,  
639 1995. A global model of natural volatile organic compound emissions. *J. Geophys. Res.*  
640 100(D5),8873–8892.

641 Guenther A.B., Jiang X., Heald C.L., Sakulyanontvittaya T., Duhl T., Emmons L.K., Wang X., 2012.  
642 The Model of Emissions of Gases and Aerosols from Nature version 2.1 (MEGAN2.1): An  
643 extended and updated framework for modeling biogenic emissions. *Geosci. Model Dev.*  
644 5(6),1471–1492. <https://doi.org/10.5194/gmd-5-1471-2012>.

645 Han Z., Zhang Y., Zhang H., Ge X., Gu D., Liu X., Bai J., Ma Z., Tan Y., Zhu F., Xia S., Du J., Tan Y., Shu  
646 X., Tang J., Sun Y., 2022. Impacts of Drought and Rehydration Cycles on Isoprene Emissions in  
647 *Populus nigra* Seedlings. *International journal of environmental research and public health*  
648 19(21). <https://doi.org/10.3390/ijerph192114528>.

649 Holopainen J.K., Gershenzon J., 2010. Multiple stress factors and the emission of plant VOCs.  
650 *Trends in plant science* 15(3),176–184. <https://doi.org/10.1016/j.tplants.2010.01.006>.

651 Jiang X., Guenther A., Potosnak M., Geron C., Seco R., Karl T., Kim S., Gu L., Pallardy S., 2018.  
652 Isoprene Emission Response to Drought and the Impact on Global Atmospheric Chemistry.  
653 *Atmospheric environment* (Oxford, England 1994) 183,69–83.  
654 <https://doi.org/10.1016/j.atmosenv.2018.01.026>.

655 Kesselmeier J., Staudt M., 1999. Biogenic Volatile Organic Compounds (VOC): An Overview on  
656 Emission, Physiology and Ecology. *Journal of Atmospheric Chemistry* 33,23–88.

657 Li Q., Gabay M., Dayan C., Misztal P., Guenther A., Fredj E., Tas E., 2024. Instantaneous intraday  
658 changes in key meteorological parameters as a proxy for the mixing ratio of BVOCs over  
659 vegetation under drought conditions. *Atmos. Chem. Phys.*

660 Li Q., Gabay M., Rubin Y., Fredj E., Tas E., 2018. Measurement-based investigation of ozone  
661 deposition to vegetation under the effects of coastal and photochemical air pollution in the

662 Eastern Mediterranean. *Science of The Total Environment* 645,1579–1597.  
663 <https://doi.org/10.1016/j.scitotenv.2018.07.037>.

664 Lionello P., 2012. *The Climate of the Mediterranean Region: From the Past to the Future*: Elsevier.

665 Llusia J., Roahtyn S., Yakir D., Rotenberg E., Seco R., Guenther A., Peñuelas J., 2016. Photosynthesis,  
666 stomatal conductance and terpene emission response to water availability in dry and mesic  
667 Mediterranean forests. *Trees* 30(3),749–759. <https://doi.org/10.1007/s00468-015-1317-x>.

668 Llusia J., Peñuelas J., 2000. Seasonal patterns of terpene content and emission from seven  
669 Mediterranean woody species in field conditions. *American J of Botany* 87(1),133–140.  
670 <https://doi.org/10.2307/2656691>.

671 Medrano H., Escalona J.M., Bota J., Gulías J., Flexas J., 2002. Regulation of photosynthesis of C3  
672 plants in response to progressive drought: Stomatal conductance as a reference parameter.  
673 *Annals of botany* 89 Spec No(7),895–905. <https://doi.org/10.1093/aob/mcf079>.

674 MIYASHITA K., TANAKAMARU S., MAITANI T., KIMURA K., 2005. Recovery responses of  
675 photosynthesis, transpiration, and stomatal conductance in kidney bean following drought  
676 stress. *Environmental and Experimental Botany* 53(2),205–214.  
677 <https://doi.org/10.1016/j.envexpbot.2004.03.015>.

678 Monson R.K., Jaeger C.H., Adams W.W., Driggers E.M., Silver G.M., Fall R., 1992. Relationships  
679 among Isoprene Emission Rate, Photosynthesis, and Isoprene Synthase Activity as Influenced  
680 by Temperature. *PLANT PHYSIOLOGY* 98(3),1175–1180.

681 Niinemets U., Loreto F., Reichstein M., 2004. Physiological and physicochemical controls on foliar  
682 volatile organic compound emissions. *Trends in plant science* 9(4),180–186.  
683 <https://doi.org/10.1016/j.tplants.2004.02.006>.

684 Niinemets U., Monson R.K., 2013. *Biology, controls and models of tree volatile organic compound*  
685 *emissions*. Dordrecht: Springer.

686 Nobel P.S., 1999. *Physicochemical & environmental plant physiology*. 2nd ed. San Diego:  
687 Academic Press.

688 Núñez L., Plaza J., Pérez-Pastor R., Pujadas M., Gimeno B.S., Bermejo V., García-Alonso S., 2002.  
689 High water vapour pressure deficit influence on *Quercus ilex* and *Pinus pinea* field  
690 monoterpene emission in the central Iberian Peninsula (Spain). *Atmospheric Environment*  
691 36(28),4441–4452. [https://doi.org/10.1016/S1352-2310\(02\)00415-6](https://doi.org/10.1016/S1352-2310(02)00415-6).

692 Owen S., Boissard C., Street R.A., Duckham S.C., Csiky O., Hewitt C.N., 1997. Screening of 18  
693 Mediterranean plant species for volatile organic compound emissions. *Atmospheric*  
694 *Environment* 31,101–117. [https://doi.org/10.1016/S1352-2310\(97\)00078-2](https://doi.org/10.1016/S1352-2310(97)00078-2).

695 Owen S.M., Hewitt C.N., 2000. Extrapolating branch enclosure measurements to estimates of  
696 regional scale biogenic VOC fluxes in the northwestern Mediterranean basin. *J. Geophys. Res.*  
697 105(D9),11573–11583. <https://doi.org/10.1029/1999JD901154>.

698 Pegoraro E., REY A.N.A., Abrell L., van HAREN J., LIN G., 2006. Drought effect on isoprene  
699 production and consumption in Biosphere 2 tropical rainforest. *Glob Change Biol* 12(3),456–  
700 469. <https://doi.org/10.1111/j.1365-2486.2006.01112.x>.

701 Peñuelas J., Munné-Bosch S., 2005. Isoprenoids: An evolutionary pool for photoprotection. *Trends*  
702 *in plant science* 10(4),166–169. <https://doi.org/10.1016/j.tplants.2005.02.005>.



703 Peñuelas J., Rutishauser T., Filella I., 2009. Ecology. Phenology feedbacks on climate change.  
704 Science (New York, N.Y.) 324(5929),887–888. <https://doi.org/10.1126/science.1173004>.  
705 Peñuelas J., Staudt M., 2010. BVOCs and global change. Trends in plant science 15(3),133–144.  
706 <https://doi.org/10.1016/j.tplants.2009.12.005>.  
707 Potosnak M.J., LeSturgeon L., Pallardy S.G., Hosman K.P., Gu L., Karl T., Geron C., Guenther A.B.,  
708 2014. Observed and modeled ecosystem isoprene fluxes from an oak-dominated temperate  
709 forest and the influence of drought stress. Atmospheric Environment 84,314–322.  
710 <https://doi.org/10.1016/j.atmosenv.2013.11.055>.  
711 Ryan A.C., Hewitt C.N., Possell M., Vickers C.E., Purnell A., Mullineaux P.M., Davies W.J., Dodd I.C.,  
712 2014. Isoprene emission protects photosynthesis but reduces plant productivity during  
713 drought in transgenic tobacco (*Nicotiana tabacum*) plants. New Phytol 201(1),205–216.  
714 <https://doi.org/10.1111/nph.12477>.  
715 Saunders S.M., Jenkin M.E., Derwent R.G., Pilling M.J., 2003. Protocol for the development of the  
716 Master Chemical Mechanism, MCM v3 (Part A): tropospheric degradation of non-aromatic  
717 volatile organic compounds. Atmos. Chem. Phys. 3,161–180.  
718 Saunier A., Ormeño E., Boissard C., Wortham H., Temime-Roussel B., Lecareux C., Armengaud A.,  
719 Fernandez C., 2017. Effect of mid-term drought on *Quercus pubescens*  
720 BVOCs' emission seasonality and their dependency on light and/or temperature. Atmos. Chem.  
721 Phys. 17(12),7555–7566. <https://doi.org/10.5194/acp-17-7555-2017>.  
722 Schade G.W., Goldstein A.H., Lamanna M.S., 1999. Are monoterpene emissions influenced by  
723 humidity? Geophys. Res. Lett. 26(14),2187–2190.  
724 Seco R., Karl T., Turnipseed A., Greenberg J., Guenther A., Llusia J., Peñuelas J., Dicken U.,  
725 Rotenberg E., Kim S., Yakir D., 2017. Springtime ecosystem-scale monoterpene fluxes from  
726 Mediterranean pine forests across a precipitation gradient. Agricultural and Forest  
727 Meteorology 237-238,150–159. <https://doi.org/10.1016/j.agrformet.2017.02.007>.  
728 Sindelarova K., Granier C., Bouarar I., Guenther A., Tilmes S., Stavrakou T., Müller J.-F., Kuhn U.,  
729 Stefani P., Knorr W., 2014. Global data set of biogenic VOC emissions calculated by the MEGAN  
730 model over the last 30 years. Atmos. Chem. Phys. 14(17),9317–9341.  
731 <https://doi.org/10.5194/acp-14-9317-2014>.  
732 Staudt M., Mandl N., Joffre R., Rambal S., 2001. Intraspecific variability of monoterpene  
733 composition emitted by *Quercus ilex* leaves. Can. J. For. Res. 31(1),174–180.  
734 <https://doi.org/10.1139/x00-153>.  
735 Street R.A., Owen S., Duckham S.C., Boissard C., Hewitt C.N., 1997. Effect of habitat and age on  
736 variations in volatile organic compound (VOC) emissions from *Quercus ilex* and *Pinus pinea*.  
737 Atmospheric Environment 31,89–100. [https://doi.org/10.1016/S1352-2310\(97\)00077-0](https://doi.org/10.1016/S1352-2310(97)00077-0).  
738 Tingey D., Turner D., Weber J., 1990. Factors Controlling the Emissions of Monoterpenes and  
739 Other Volatile Organic Compounds: U.S. Environmental Protection Agency, Washington, D.C.  
740 EPA/600/D-90/195 (NTIS PB91136622).  
741 Vilagrosa A., Bellot J., Vallejo V.R., Gil-Pelegrin E., 2003. Cavitation, stomatal conductance, and  
742 leaf dieback in seedlings of two co-occurring Mediterranean shrubs during an intense drought.  
743 Journal of experimental botany 54(390),2015–2024. <https://doi.org/10.1093/jxb/erg221>.